We are IntechOpen, the world's leading publisher of Open Access books Built by scientists, for scientists

4,800
Open access books available

122,000
International authors and editors

135M
Downloads

Our authors are among the

154
Countries delivered to

TOP 1%
most cited scientists

12.2%
Contributors from top 500 universities

CLARIVATE ANALYTICS BOOK CITATION INDEX INDEXED

WEB OF SCIENCE™

Selection of our books indexed in the Book Citation Index in Web of Science™ Core Collection (BKCI)

Interested in publishing with us?
Contact book.department@intechopen.com

Numbers displayed above are based on latest data collected.
For more information visit www.intechopen.com

15

Quantum Computation with Graphene Nanostructure

Zhi-Rong Lin, Guo-Ping Guo, Tao Tu, Qiong Ma and Guang-Can Guo
Key Laboratory of Quantum Information, University of Science and Technology of China, Chinese Academy of Sciences, Hefei, 230026 P.R.China

1. Introduction

Quantum computers which can efficiently simulate complex quantum systems and solve certain classes of hard mathematical problems are of great interest and importance. However, practical implementation of a large-scale quantum computer represents a formidable challenge. One significant obstacle is combining good access to the quantum system with high degree isolation from the environment in a scalable system.

The spin qubit proposal is a promising approach to address the central issues (Loss et al., 1998). The electron spin is a two-level system which is a natural candidate for realization of a quantum bit. Spin qubits in semiconductor nanostructures can be accessed and scaled easily. After the original spin-qubit proposal, there has been enormous research effort in implementing the spin-based information processing and the major breakthroughs in basic proof-of-principle experiments have been achieved in GaAs/AlGaAs quantum dots. First, the single-shot measurement of an individual electron spin has been realized (Elzerman et al., 2004). Second, the demonstrations of the $\sqrt{SWAP}$-gate on two-electron spin states (Petta et al., 2005) and single spin rotations (Koppens et al., 2006; Nowack et al., 2007; Pioro-Ladrière et al., 2008) suffice to universal quantum operations of spin qubits. By now all parts of the original Loss-DiVincenzo proposal have been demonstrated in the proof-of-principle experiments. To build a scalable quantum computer requires that the gate error should be smaller than the threshold and the decoherence time should be 10^4 times longer than the operation time. However because of interaction with the nuclei environment in the host GaAs/AlGaAs material via both lattice-mediated spin-orbit interactions and hyperfine interactions, the decoherence times are not long enough compared to the single qubit operations. Because of the completely eliminated hyperfine interactions in graphene, there is great potential for electron spin qubits in a nuclear-spin-free quantum world (Trauzettel et al., 2007). It is highly desirable to propose an efficient architecture made with graphene nanostructures to implement the quantum information processing (QIP) (Pedersen et al., 2008).

Owing to the special band structure of graphene (Castro Neto et al., 2009), its low-energy quasi-particles behave as Dirac fermions, and the Klein tunneling and Chiral effect make it non-trivial to form well controllable quantum dots in graphene. There are several ways in which one could localize electrons (holes) in graphene; by using suitable transverse states in Graphene nanoribbon (GNR) (Trauzettel et al., 2007; Silvestrov et al., 2007), by electrical confinement in bilayer graphene (Peeters et al., 2007), or by using the topological structure

(Wang et al., 2007). In the chapter, we propose two alternative approaches that the localized states can exist in the zigzag region of a GNR with a sequence of Z-shaped structures (Guo et al., 2009) or substrate modulated graphene quantum dot (Ma et al., 2009). The localized electron (hole) spin states can be used, as the physical qubit. For the GNR quantum dot chain, the interaction between qubits is found to be of the always-on Heisenberg form. Moreover, for a practical quantum computer to operate, it is essential to properly tailor the disturbing environment. An important technique for doing this is the use of quantum bang-bang (BB) control strategy and the decoherence-free subspaces (DFS) encoding method, both of which are traditionally discussed in the context of atomic, molecular and optical setup (Morton et al., 2006; Kwiat et al., 2000; Kielpinski et al., 2001; Viola et al., 2001; Zhang et al., 2004). In this chapter, these ideas will be introduced to construct an effective quantum information circuit in new graphene nanostructure below.

2. Electron localization in graphene quantum dots

2.1 Quantum dots on a graphene nanoribbon

It is difficult to form a conventional-type quantum dot inside an infinite graphene because of Klein tunneling which wound induce charge transmission through the interface of p-n junctions. Trauzettel, Bulaev, Loss and Burkard firstly introduced a method to overcome such difficulties and form spin qubits in quantum dots based on GNR with armchair boundaries in 2007 (Trauzettel et al., 2007). For the semiconducting armchair boundary conditions, both sublattices of graphene's hexagonal structure will be terminated equally on both side which result in the emergence of a gap and destruction of the valley degeneracy. The charge carriers can be confined on the quantum dot regions between two barrier regions in which electric potential can be tuning by applying a appropriate local gate voltage. Since all the bound states are non-degenerate in valley space, the spin qubits are proposed in this graphene nanostructure. The two spin qubits are coupled via an exchange coupling and the exchange coupling is controlled by the tunnel barrier between the dots. In combination with single spin operations, universal quantum gates can be achieved. The interest idea of the proposal is non-local electron spins in any two of dots can be coupled with the others being decoupled by detuning. Therefore long-distance quantum gates in graphene quantum dots are feasible.

2.2 Substrate modulated graphene quantum dot

In this section, we concentrate on a new method to use gapped graphene as barrier to confine electrons in gapless graphene and form a good quantum dot, which can be realized on an oxygen-terminated SiO_2 substrate partly H-passivated. Further, this method can be upgraded to form two-dimensional quantum dot arrays. We systematically investigate two-dimensional system and find that the coupling strength between neighboring dots can be uniquely anisotropic. The ability to achieve more complex and scalable pattern in our proposal suffice to design a large-scale quantum computer in principle.

Recently, it was discussed that the electronic energy spectrum of the monolayer graphene depended strongly on the surface characteristic of the substrate (Zhou et al., 2007; Shemella et al., 2009). For example, if a single layer graphene is deposited onto a SiO_2 surface, a finite energy gap will open between conduction and valence bands for an oxygen-terminated surface, but close when the oxygen atoms on the substrate are passivated with hydrogen atoms. The confinement can be achieved by a gapless nanoscale graphene regions connecting with gapped regions, which serve as barriers, as shown in Fig 1. The devices are realizable in experiment. In an oxygen terminated SiO_2 substrate, we use protective stuff to cover the

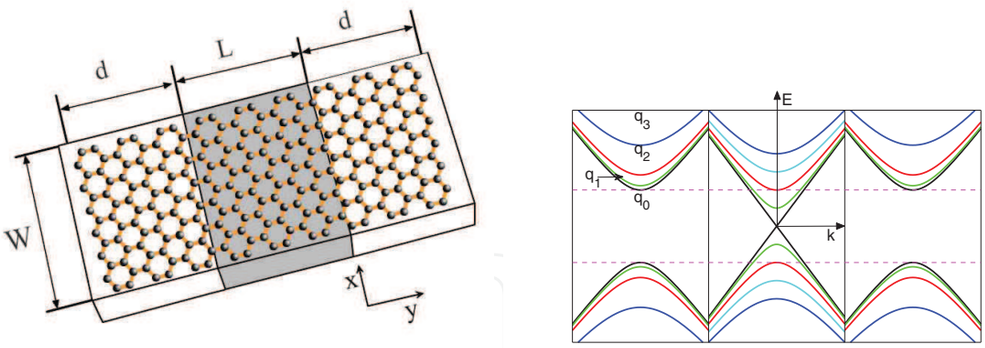

(a) (b)

Fig. 1. (a) Schematic of a single quantum dot. A GNR is deposited on a SiO_2 substrate. The dark part is the dot region, which is fully hydrogen-passivated and gapless. The light part is the barrier region, which is non hydrogen-passivated or slightly hydrogen-passivated and gapped. (b) Energy bands of this system.

barrier regions and the dot region is fully exposed to hydrogen atoms atmosphere. Then a single layer graphene is deposited on this substrate and the bound states exit in the hydrogen-passivated regions. Compared to the approach of forming quantum dots on GNR with semiconducting armchair boundary conditions (Trauzettel et al., 2007), the realization of quantum dot will not depend much on the boundary conditions. Since ferromagnetic insulators deposited on graphene can induce ferromagnetic correlations in graphene, we consider adding ferromagnetic insulator such as EuO upon the two gapped graphene barriers. The induced exchange interaction is estimated to achieve 5 meV by using EuO (Haugen et al., 2008).

The electron waves in graphene system are usually described by four component spinor envelop wavefunction $\Psi = (\psi_A^{(K)}, \psi_B^{(K)}, -\psi_A^{(K')}, -\psi_B^{(K')})$. The behaviors of low energy electron can be described by 4×4 Dirac equation for massless or massive particles, which can be written as (Recher et al., 2009): in the dot region (where $0 \leq y \leq L$),

$$-i\hbar v_F \begin{pmatrix} \sigma_x\partial_x + \sigma_y\partial_y & 0 \\ 0 & -\sigma_x\partial_x + \sigma_y\partial_y \end{pmatrix} \Psi = E\Psi, \tag{1}$$

and in the barrier region (where $y < 0$ or $y > L$),

$$-i\hbar v_F \begin{pmatrix} \sigma_x\partial_x + \sigma_y\partial_y & 0 \\ 0 & -\sigma_x\partial_x + \sigma_y\partial_y \end{pmatrix} \Psi + \Delta \begin{pmatrix} \sigma_z & 0 \\ 0 & \sigma_z \end{pmatrix} \Psi - \eta V_\sigma \Psi = E\Psi, \tag{2}$$

where $\hbar$ is the Planck constant, $v_F \approx 10^6$ m/s is the Fermi velocity, σ_x, σ_y, σ_z are Pauli matrices acting on two-spinor states related to the two triangular sublattices of graphene, $\eta = \pm 1$ stands for the two spin indexes (spin up and spin down). 2Δ is the gap induced by the substrate, $2V_\sigma$ is the spin splitting energy due to the correlation with ferromagnetic contacts. We consider metallic armchair shaped GNR with the quantized transverse momentum $q_n = n\frac{\pi}{W}$ and the wave vectors in the y direction should satisfy different conditions as

$$E = \pm\sqrt{(\hbar v_F q_n)^2 + (\hbar v_F k)^2}, \tag{3}$$

in the dot and

$$E = \pm\sqrt{(\hbar v_F q_n)^2 + (\hbar v_F k')^2 + \Delta^2} - \eta V_\sigma, \tag{4}$$

in the barriers, where k is the wave vector in the dot and $k^{'}$ in the ferromagnetic barrier with $\pm$ signs referring to conduction band $(+)$ and valence band $(-)$ respectively. The bound state requires that $k^{'}$ is a pure imaginary, which means the bound state energy should satisfy

$$|E| \geqslant \hbar v_F |q_n|,\ |E + \eta V_\sigma| < \sqrt{(\hbar v_F q_n)^2 + \Delta^2}. \tag{5}$$

The energy levels of the bound states can be obtained by matching the wavefunctions at $y = 0$ and $y = L$. We use $1/L$ as the unit of q_n and the characteristic energy $\hbar v_F/L$ as the energy unit. In Fig. 2, we show the energy spectrum as a function of the substrate induced interaction Δ for different transverse momentums (q_n) where V_σ is assumed to be 5 meV (Haugen et al., 2008). As shown in Fig. 2, when Δ increases, the number of bound states is increasing at the same time, which can be deduced from Eq. 5.

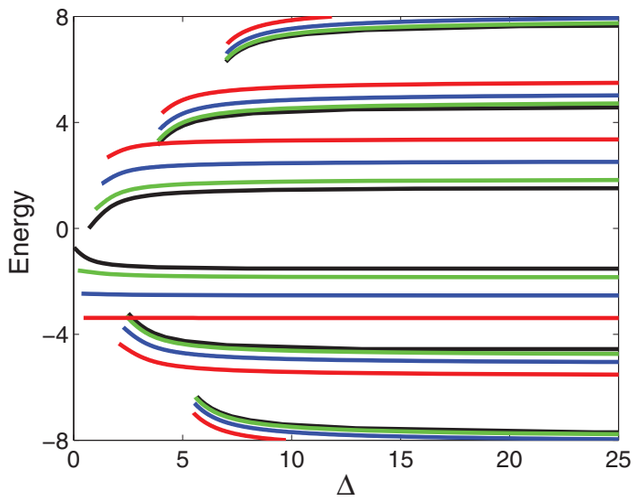

Fig. 2. Bound-state energy levels of a substrate modulated graphene quantum dot with $V_\sigma = 5meV$ for $q_n = 0, 1, 2, 3$ and $\eta = 1$, black: $q_n = 0$, green: $q_n = 1$, blue: $q_n = 2$, red: $q_n = 3$. Both axe labels are in the characteristic energy unit of $\hbar v_F/L$. The length L and width W of dot are assumed to be 100 nm and 300 nm respectively.

Our approach can be easily developed to more complex and scalable pattern. Here we study a two-dimensional quantum dot array as shown in Fig. 3a. Instead of forming transverse modes of nanoribbon, the wavefunctions must match between dot and barrier along both x and y directions. The energy spectrum of this system has been plotted in Fig. 3b. The neighboring dots are coupled by the exchange coupling J. We obtain J by calculating the exchange coupling $J = 4t^2/U$ according to Hubbard approximation. Here U is onsite Coulomb energy and $t = \varepsilon \int \varphi_1^\dagger(\vec{r_1})\varphi_2(\vec{r_2})$ is tunnelling matrix element between two neighboring quantum dots, where ε is the single-particle bound state energy and $\varphi_1(\vec{r})$ and $\varphi_2(\vec{r})$ are the wavefunctions of two neighboring or next-nearest neighboring dots. We estimate $U \approx 10$ meV for the dot size $L \approx 30$ nm and the characteristic energy unit of this system $\hbar v_F/L$ is about 22 meV. Fig. 4 shows the nearest coupling strength (J_1) and the next-nearest coupling strength (J_2) of the ground state versus the opened gap Δ in the barrier region (when $d = 3L$), from which we

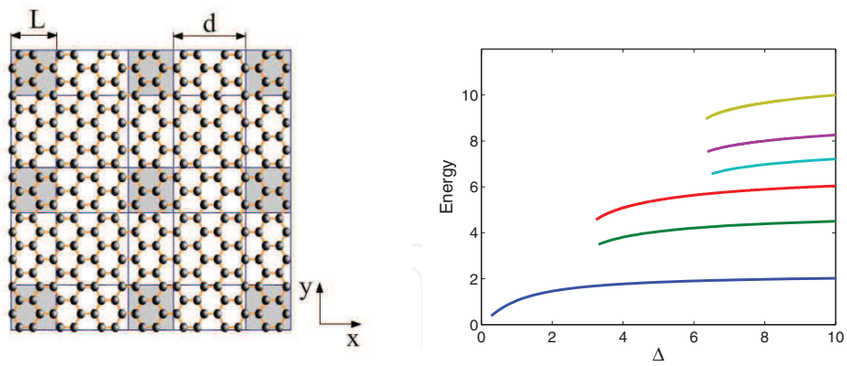

(a) (b)

Fig. 3. (a) Schematic drawing of two-dimensional quantum dot arrays. The dot regions (dark regions) are defined by the gapped barrier regions (light regions). (b) The bound-state energy levels of this two-dimensional system with $L = 30$ nm and $d = 3L$. Both axe labels are in the characteristic energy unit of $\hbar v_F / L$.

find that the nearest coupling strength decreases sharply when the opened gap increases. We also find that the nearest coupling both along the x direction and y direction are the same for the ground state, and coupling strengths between the nearest and next-nearest neighboring dots are anisotropic for excited states.

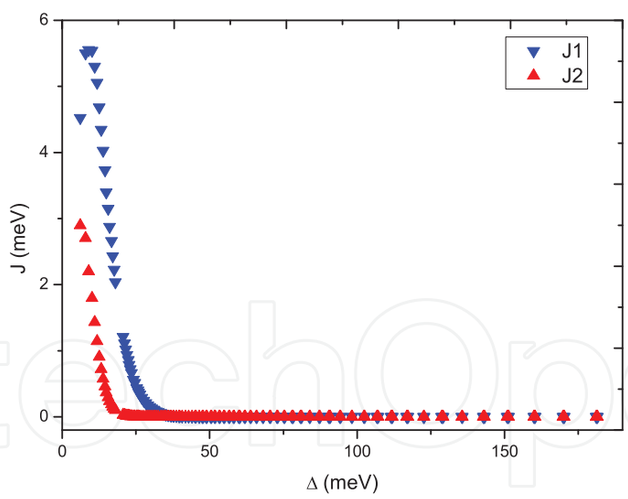

Fig. 4. Coupling strength of the nearest (J_1) and next-nearest (J_2) dots as a function of the opened gap Δ in the barrier region for the ground state.

2.3 Graphene nanoribbon quantum dot chain

In this section, we introduce a graphene quantum system in which the proposed GNR consists of an array of Z-shaped structures and each Z-shaped structure includes a central region with zigzag edge connecting to two regions with armchair edge, as presented in Fig. 5d.

Using the π orbital tight-binding(TB) approximation, the density of states and the spectrum of the zigzag region in this GNR system can be obtained by the direct diagonalization with periodic boundary conditions. We find that there are several localized states with electron-hole symmetry around the zero energy point, as shown in Fig.5a. Considering higher-order hopping terms, we calculated the DOS and the spectrum using a third nearest-neighbor TB model instead of nearest-neighbor TB model with the second and third neighbor interaction energies $\gamma_1 = -0.12$eV and $\gamma_2 = -0.068$eV (Reich et al., 2002; Son et al., 2006). As shown in Fig. 5a and Fig. 6, higher-order hopping terms destroy the electron-hole symmetry, but don't destroy the confined states in each zigzag region. Hence we can choose to get one localized electron or hole in the zigzag region by adjusting the Fermi level through the individual top gates. Furthermore, in the calculations we find that the spectrum of GNR depends very much on the nature of their geometry. There are no localized states in the zigzag regions when the width of this GNR $N = 3m - 1$ or $N = 2m$ (unit cells), as shown in Fig. 6. Here m is an integer. We now discuss two coupled Z-shaped quantum dots, which are connected with armchair GNR. Fig. 5b shows the spatial distribution of local probability density of a typical GNR with two Z-shaped structures, and $N = 7$, $L = 4$, $D = 6$ for $E_0 = \pm 0.3$ eV discrete states. As shown in Fig. 5c, each zigzag region (quantum dot) confines one electron and these two electrons are coupled by the exchange interaction J_1. J_1 can be obtained by calculating the exchange interaction $J_1 = 4t^2/U$. Obviously, the exchange coupling J_1 is determined by the geometry of the nanoribbon. For each N and L, J_1 depends on the distance between two neighboring dots D (unit cells), as shown in Fig. 7.

The spin of the localized charge carrier is used as the physical qubit and the GNR with a sequence of Z-shaped structures forms an one-dimensional spin qubit chain as shown in Fig. 5d. In this chapter, we neglect the magnetic effect of GNR edge (Son et al., 2009). The neighboring qubits in this chain have an always-on Heisenberg interaction $H = J_1 \vec{S_1} \cdot \vec{S_2}$. Here $\vec{S_1}$ and $\vec{S_2}$ are the spin operators of the neighboring localized charge carrier. For a sequence of Z-shaped structure GNR with parameters as $N = 7$, $L = 4$, $D = 18$, the Hamiltonian of the system can be expressed as

$$H_I = \sum_{\langle i,j \rangle} J_{i,j} (\sigma_i^x \otimes \sigma_j^x + \sigma_i^y \otimes \sigma_j^y + \sigma_i^z \otimes \sigma_j^z), \tag{6}$$

where $\sigma_{i,j}^{x,y,z}$ are the spin Pauli operators of the localized charge carrier in the quantum dots, $\langle i, j \rangle$ represent two nearest neighboring dots.

3. Quantum-noise control in graphene nanoribbon quantum dot chain

The main challenges for solid-state QIP are achieving the high accuracy of gate operation and tailoring the disturbing environment. In our one-dimensional spin qubit chain, the quantum information is disturbed by the charge noise, the nuclear spins in substrate and inherent spin-spin interaction. Therefore achieving noise control is indispensable. A variety of strategies have been devised to meet this challenge, no single method can suppress the complex noise and decoherence. Rather, constructing a reliable QIP scheme depends crucially on the errors that happen. First, to avoid the spin qubits to entangle with the environment, we can apply a BB operation $U_z = exp(-i\sigma_z \pi/2)$ to each quantum dot region. Such rotation operations can be implemented through the electrically driven single-electron spin resonance by localized a.c. electric field pulses if ferromagnetic strips are integrated on top of the graphene quantum dots, which has been successfully realized in GaAs/AlGaAs quantum dot

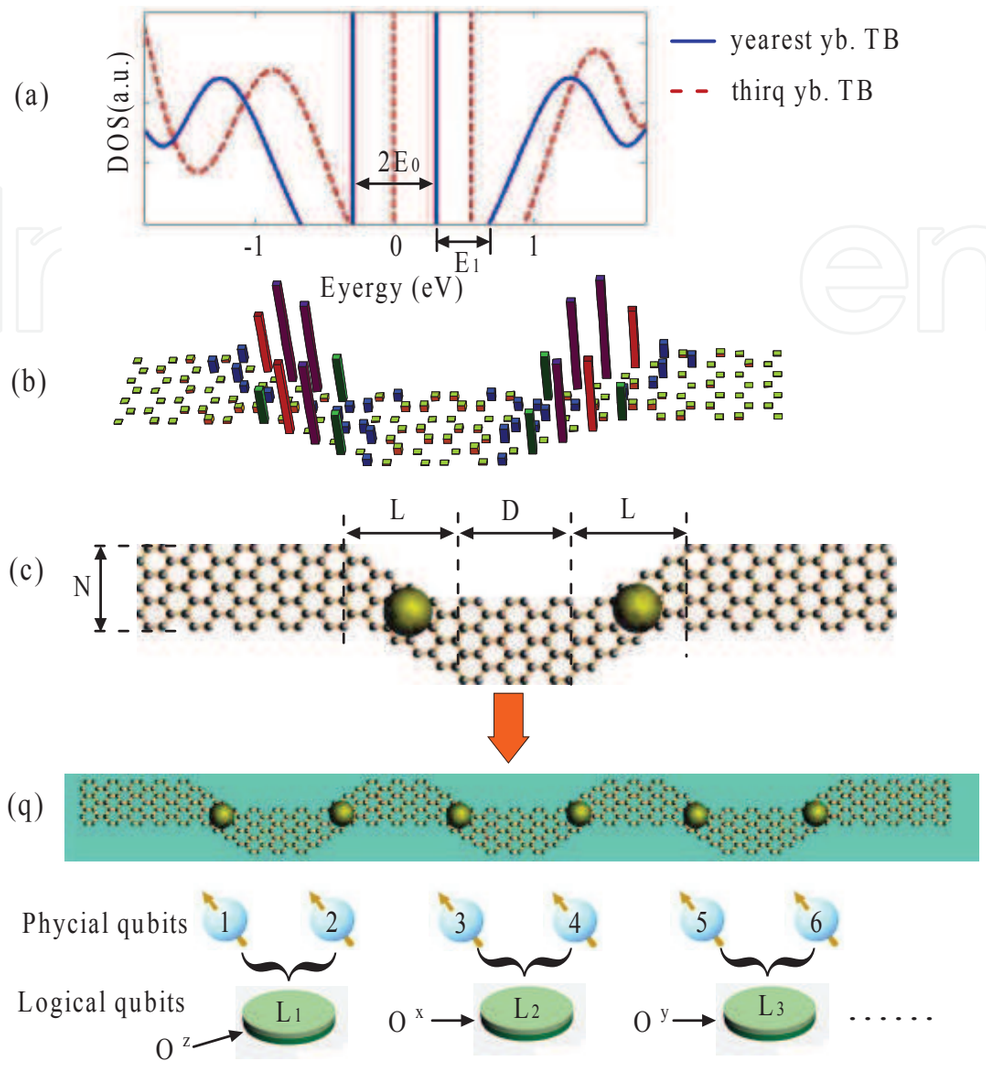

Fig. 5. Schematic illustration of the proposed architecture of GNR quantum dot chain. (a) The density of states of the GNR are calculated by nearest neighbor TB approximation and third nearest-neighbor TB approximation with the second and third neighbor interaction energies $\gamma_1 = -0.12$eV and $\gamma_2 = -0.068$eV. (b) The spatial distribution of local probability density of GNR with two coupled quantum dots, and $N = 7$, $L = 4$, $D = 6$ for ground states. (c) Two coupled graphene quantum dots in which each dot is filled with a single electron. The physical qubit is encoded into the spin of the confined electron. (d) The proposed periodic architecture with three logical qubits as a unit for quantum computation. Physical qubits 1 and 2 form logical qubit L_1; physical qubits 3 and 4 form logical qubit L_2; physical qubits 5 and 6 form logical qubit L_3. The G^z , G^x, G^y are the BB operation sets of L_1, L_2 and L_3 respectively. The cyan ribbon indicates the micromagnet integrated on top of the GNR structure to apply an slanting magnetic field. The GNR and micromagnet are isolated by an insulating layer. Each zigzag region has a nearby gate. The nearby gates are not outlined for clarity.

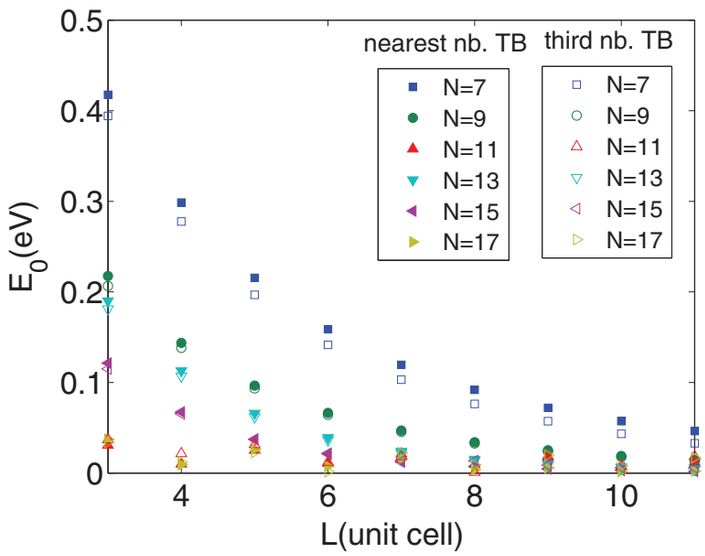

Fig. 6. The ground-state energy E_0 of the quantum dot in the GNR chain versus length of quantum dot region L (unit cells) for different width of the nanoribbon N (unit cells).

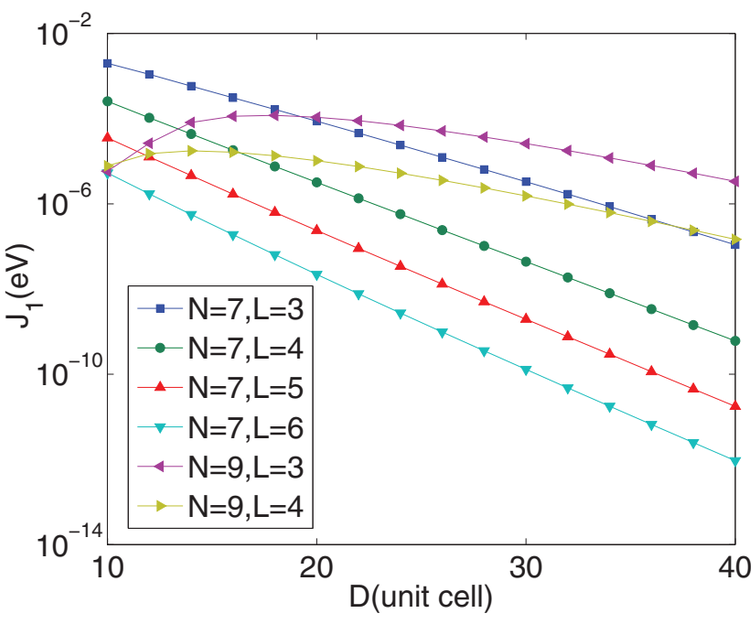

Fig. 7. The coupling energy J_1 of two nearest neighboring dots in GNR quantum dot chain versus the distance between two dots D (unit cells) for different size of quantum dot region.

experiment recently (Pioro-Ladrière et al., 2008). Next, to counteract the phase decoherence, we can use DFS encoding (Duan et al., 1997; Lidar et al., 1998; Benjamin et al., 2003). For a simply DFS encoding, two physical qubits can encode a logical qubit:

$$|0\rangle_L = |\uparrow_1\downarrow_2\rangle, |1\rangle_L = |\downarrow_1\uparrow_2\rangle. \tag{7}$$

As shown in Fig. 5c, localized electron spins in the two neighboring zigzag regions can be used to form a logical qubit.

Furthermore, a special encoding method and a nonsynchronous BB pulse operations are exploited to overcome the untunable spin-spin interactions between two neighboring physical qubits (Zhang et al., 2004). We proposed a GNR quantum dot chain architecture, which forms a periodic structure $L_1L_2L_3L_1L_2L_3\cdots$ with three logical qubits as a unit, as shown in Fig. 5d. L_1 represents a logical qubit encoded as Eq. (7). L_2 is a logical qubit encoded as

$$|0\rangle_{L2} = \frac{1}{2}(|\uparrow\rangle_3 + |\downarrow\rangle_3)(|\uparrow\rangle_4 - |\downarrow\rangle_4), \tag{8}$$

$$|1\rangle_{L2} = \frac{1}{2}(|\uparrow\rangle_3 - |\downarrow\rangle_3)(|\uparrow\rangle_4 + |\downarrow\rangle_4). \tag{9}$$

And L_3 is a logical qubit encoded as

$$|0\rangle_{L3} = \frac{1}{2}(|\uparrow\rangle_5 + i|\downarrow\rangle_5)(|\uparrow\rangle_6 - i|\downarrow\rangle_6), \tag{10}$$

$$|1\rangle_{L3} = \frac{1}{2}(|\uparrow\rangle_5 - i|\downarrow\rangle_5)(|\uparrow\rangle_6 + i|\downarrow\rangle_6). \tag{11}$$

With this periodic architecture, we need to apply nonsynchronous BB pulse operations respectively to L_1, L_2, L_3 from the operation sets $G^z = \{I, U_z, R_z\}$, $G^x = \{I, U_x, R_x\}$, $G^y = \{I, U_y, R_y\}$, where $U_z = -\sigma_1^z \otimes \sigma_2^z$, $R_z = -iI_1^z \otimes \sigma_2^z$, $U_x = -\sigma_1^x \otimes \sigma_2^x$, $R_x = -iI_1 \otimes \sigma_2^x$, $U_y = -\sigma_1^y \otimes \sigma_2^y$, and $R_y = -iI_1 \otimes \sigma_2^y$. Thus we obtain a quantum computation system with entirely decoupled logical qubits.

4. Universal quantum gates in GNR quantum dot chain

In this section, we discuss the scheme to perform universal set of quantum gates on encoded qubits. Since arbitrary single-qubit rotations can be constructed from the two elementary logic operations $\bar{X}$ and $\bar{Z}$, we show how to implement the two gate operations in the GNR quantum dot chain. For logical qubit L_1, $\bar{X} = \frac{1}{2}(\sigma_1^x \otimes \sigma_2^x + \sigma_1^y \otimes \sigma_2^y)$, $\bar{Z} = \frac{1}{2}(\sigma_1^z - \sigma_2^z)$. $\bar{X}$ gate can be easily achieved by adjusting the BB pulses of both qubits 1 and 2 to be synchronous. The operation time is $\Delta t = \hbar\pi/4J = 0.2$ ns, for $N = 7$, $L = 4$, $D = 18$. $\bar{Z}$ gate can be achieved by localized pluses on the two physical qubits respectively. The operation time of $\bar{Z}$ gate can be nanosecond scale when a slanting magnetic field with large field gradient is applied onto each quantum dot region (Pioro-Ladrière et al., 2008). The fidelity of the $\bar{X}$ gate is limited by fluctuations in the qubit splitting J caused by charge noise, such as $1/f$ noise. The accuracy of the $\bar{Z}$ gate is dominated by spin dephasing due to the nuclear field fluctuations. The fidelity of the $\bar{Z}$ gate can be very high due to the small nuclear field in graphene system.

Combined with the arbitrary single-qubit rotation, two-qubit CNOT gate on any two logical qubits is required to complete our universal set of quantum gates. For example, we construct CNOT gate between two neighboring logical qubits, L_1 and L_2. It is shown that CNOT gate can be implemented by W gate $W = e^{i\theta\bar{Z}\otimes\bar{Z}}$ conjugating Hadamard operation. It has been

known that W gate is equivalent to a controlled rotation about the z axis: $W = e^{i\theta \bar{Z}\otimes\bar{Z}} = |0\rangle\langle 0| \otimes I + |1\rangle\langle 1| \otimes e^{2i\theta\bar{Z}}$ (Bremner et al., 2002). By performing Hadamard transformation to the two physical qubits of the second logical qubit L_2 and changing the BB control pulse to be the same with L_1, we can recouple the two neighboring logical qubits and implement W gate of logical qubits of L_1 and L_2.

The spin decoherence time of graphene quantum dot has been predicted to be more than 10 μs in the nature carbon material (Trauzettel et al., 2007; Fischer et al., 2009). This decoherence time is 4 orders longer than the gate operation time of the present scheme and the gate error might meet the required threshold in principle. This combined DFS and BB control method is a useful approach to offer the possibility for coherent controlling spin qubits on graphene.

5. Conclusion

To conclude, we have discussed the potential to implement spin-based quantum computation on graphene nanostructures. Several approaches have been introduced to achieved quantum confinement of charge carriers. To overcome the dependence on the boundary conditions of GNR, we proposed a method to form quantum dots in substrate modulated graphene. We presented the theoretical proposals for forming logical qubit encoding in a DFS subspace and achieving noise control by BB control strategy in a GNR quantum dot chain with always-on Heisenberg interaction. Furthermore, universal set of quantum gates on encoded qubits has been achieved by a sequence of pulse control. Recently, the experimental breakthroughs in few electrons or holes graphene quantum dots (Neubeck et al., 2010) open an avenue for realization of spin qubit in graphene nanostructure.

6. Acknowledgments

This work was supported by the National Science Foundation (ECS-0601478), the National Basic Research Program of China (Grants No. 2011CBA00200), and the National Natural Science Foundation of China (Grants 10804104, 10874163, and 10934006).

7. References

Loss D. & DiVincenzo D. P. (1998). Quantum computation with quantum dots, *Physical Review A*, Vol. 57, Issue 1, pp. 120-126.

Elzerman J. M.; Hanson R.; Willems Van Beveren L. H.; Witkamp B.; Vandersypen L. M. & Kouwenhoven L. P. (2004). Single-shot read-out of an individual electron spin in a quantum dot, *Nature*, Vol. 430, No. 6998, pp. 431-435.

Petta J. R.; Johnson A. C.; Taylor J. M.; Laird E. A.; Yacoby A.; Lukin M. D.; Marcus C. M.; Hanson M. P. & Gossard A. C. (2005) Coherent manipulation of coupled electron spins in semiconductor quantum dots, *Science*, Vol. 309, No. 5744, pp. 2180-2184.

Koppens F. H.; Buizert C.; Tielrooij K. J.; Vink I. T.; Nowack K. C.; Meunier T.; Kouwenhoven L. P. & Vandersypen L. M. (2006) Driven coherent oscillations of a single electron spin in a quantum dot, *Nature*, Vol. 442, No. 7104, pp. 766-771.

Nowack K. C.; Koppens F. H. L.; Nazarov Yu. V. & Vandersypen L. M. K. (2007) Coherent control of a single electron spin with electric fields , *Science*, Vol. 318, No. 5855, pp. 1430-1433.

Pioro-Ladrière M.; Obata T.; Tokura Y.; Shin Y. S.; Kubo T.; Yoshida K.; Taniyama T. & Tarucha S. (2008) Electrically driven single-electron spin resonance in a slanting Zeeman field, *Nature Physics*, Vol. 4, Issue 10, pp. 776-779.

Trauzettel B.; Bulaev D. V.; Loss D. & Burkard G. (2007) Spin qubits in graphene quantum dots, *Nature Physics*, Vol. 3, Issue 3, pp. 192-196.

Pedersen T. G.; Flindt C.; Pedersen J.; Mortensen N. A.; Jauho A. P. & Pedersen K. (2008) Graphene antidot lattices: designed defects and spin qubits, *Physical Review Letters*, Vol. 100, Issue 13, pp. 136804.

Castro Neto A. H.; Guinea F.; Peres N. M. R.; Novoselov K. S. & Geim A. K. (2009) The electronic properties of graphene, *Reviews of Modern Physics*, Vol. 81, Issue 1, pp. 109-162.

Silvestrov P. G. & Efetov K. B. (2007) Quantum dots in graphene, *Physical Review Letters*, Vol. 98, Issue 1, pp. 016802.

Pereira J. M. Jr.; Vasilopoulos P.; & Peeters F. M. (2007) Tunable quantum dots in bilayer graphene, *Nano Lett.*, Vol. 7, Issue 4, pp. 946-949.

Wang Z. F.; Shi Q. W.; Li Q. X.; Wang X. P.; Hou J. G.; Zheng H. X.; Yao Y. & Chen J. (2007) *Applied Physics Letters*, Vol. 91, Issue 5, pp. 053109.

Guo G. P.; Lin Z. R.; Tu T.; Cao G.; Li X. P. & Guo G. C. (2009) Quantum computation with graphene nanoribbon, *New Journal of Physics*, Vol. 11, pp. 123005.

Ma Q.; Lin Z. R.; Tu T.; Guo G. C. & Guo G. P.(2009) Substrate modulated graphene quantum dot, *arxiv*, 0910.4708.

Morton J. J. L.; Tyryshkin A. M.; Ardavan A.; Benjamin S. C.; Porfyrakis K.; Lyon S. A. & Briggs G. A. D. (2006) Bang-bang control of fullerene qubits using ultrafast phase gates, *Nature Physics*, Vol. 2, Issue 1, pp. 40-43.

Kwiat P. G.; Berglund A. J.; Altepeter J. B. & White A. G. (2000) Experimental Verification of Decoherence-Free Subspaces, *Science*, Vol. 290, No. 5491, pp. 498-501.

Kielpinski D.; Meyer V.; Rowe M. A.; Sackett C. A.; Itano W. M.; Monroe C. & Wineland D. J. (2001) A Decoherence-Free Quantum Memory Using Trapped Ions, *Science*, Vol. 291, No. 5506, pp. 1013-1015.

Viola L.; Fortunato E. M.; Pravia M. A.; Knill E.; Laflamme R. & Cory D. G. (2001) Experimental realization of noiseless subsystems for quantum information processing, *Science*, Vol. 293, No. 5537, pp. 2059-2063.

Zhang Y.; Zhou Z. W.; Yu B. & Guo G. C. (2004) Concatenating dynamical decoupling with decoherence-free subspaces for quantum computation, *Physical Review A*, Vol. 69, Issue 4, pp. 042315.

Zhou S. Y.; Gweon G.-H.; Fedorov A. V.; First P. N.; de Heer W. A.; Lee D.-H.; Guinea F.; Castro Neto A. H. & Lanzara A. (2007) Substrate-induced bandgap opening in epitaxial graphene, *Nature Materials*, Vol. 6, Issue 10, pp. 770-775.

Shemella P. & Nayak S. K. (2009) Electronic structure and band-gap modulation of graphene via substrate surface chemistry, *Applied Physics Letters*, Vol. 94, Issue 3, pp. 032101.

Recher P.; Nilsson J.; Burkard G. & Trauzettel B. (2009) Bound states and magnetic field induced valley splitting in gate-tunable graphene quantum dots *Physics Reiview B*, Vol. 79, Issue 8, pp. 085407.

Haugen H.; Huertas-Hernando D. & Brataas A. (2008) Spin transport in proximity-induced ferromagnetic graphene, *Physics Reiview B*, Vol. 77, Issue 11, pp. 115406.

Reich S.; Maultzsch J. & Thomsen C. (2002) Tight-binding description of graphene, *Physics Reiview B*, Vol. 66, Issue 3, pp. 035412.

Son Y. W.; Cohen M. L. & Louie S. G. (2006) Energy gaps in graphene nanoribbons, *Physics Reiview Letters*, Vol. 97, Issue 21, pp. 216803.

Muñoz-Rojas F.; Fernández-Rossier J. & Palacios J. J. (2009) Giant magnetoresistance in ultrasmall graphene based devices, *Physics Reiview Letters*, Vol. 102, Issue 13, pp. 136810.

Duan L. M. & Guo G. C. (1997) Preserving coherence in quantum computation by pairing quantum bits, *Physics Reiview Letters*, Vol. 79, Issue 10, pp. 1953-1956.

Lidar D. A.; Chuang I. L. & Whaley K. B. (1998) Decoherence-free subspaces for quantum computation, *Physics Reiview Letters*, Vol. 81, Issue 12, pp. 2594-2597.

Benjamin S. C. & Bose S. (2003) Quantum computing with an always-On Heisenberg interaction, *Physics Reiview Letters*, Vol. 90, Issue 24, pp. 247901.

Bremner M. J.; Dawson C. M.; Dodd J. L.; Gilchrist A.; Harrow A. W.; Mortimer D.; Nielsen M. A. & Osborne T. J. (2002) Practical scheme for quantum computation with any two-Qubit entangling gate, *Physics Reiview Letters*, Vol. 89, Issue 24, pp. 247902.

Fischer J.; Trauzettel B. & Loss D. (2009) Hyperfine interaction and electron-spin decoherence in graphene and carbon nanotube quantum dots, *Physics Reiview B*, Vol. 80, Issue 15, pp. 155401.

Neubeck, S.; Ponomarenko, L. A.; Freitag, F.; Giesbers, A. J. M.; Zeitler, U.; Morozov, S. V.; Blake, P.; Geim, A. K. & Novoselov, K. S. (2010). From One Electron to One Hole: Quasiparticle Counting in Graphene Quantum Dots Determined by Electrochemical and Plasma Etching, *Small*, Vol. 6, Issue 14, pp. 1469-1473.

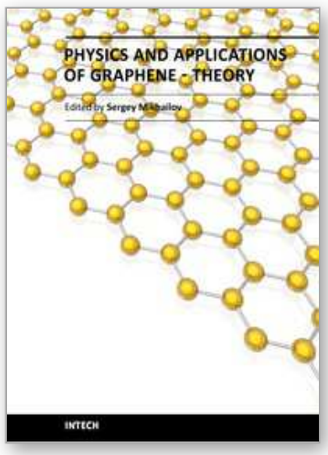

Physics and Applications of Graphene - Theory

Edited by Dr. Sergey Mikhailov

ISBN 978-953-307-152-7
Hard cover, 534 pages
Publisher InTech
Published online 22, March, 2011
Published in print edition March, 2011

The Stone Age, the Bronze Age, the Iron Age... Every global epoch in the history of the mankind is characterized by materials used in it. In 2004 a new era in material science was opened: the era of graphene or, more generally, of two-dimensional materials. Graphene is the strongest and the most stretchable known material, it has the record thermal conductivity and the very high mobility of charge carriers. It demonstrates many interesting fundamental physical effects and promises a lot of applications, among which are conductive ink, terahertz transistors, ultrafast photodetectors and bendable touch screens. In 2010 Andre Geim and Konstantin Novoselov were awarded the Nobel Prize in Physics "for groundbreaking experiments regarding the two-dimensional material graphene". The two volumes Physics and Applications of Graphene - Experiments and Physics and Applications of Graphene - Theory contain a collection of research articles reporting on different aspects of experimental and theoretical studies of this new material.

InTech Europe
University Campus STeP Ri
Slavka Krautzeka 83/A
51000 Rijeka, Croatia
Phone: +385 (51) 770 447
Fax: +385 (51) 686 166
www.intechopen.com

InTech China
Unit 405, Office Block, Hotel Equatorial Shanghai
No.65, Yan An Road (West), Shanghai, 200040, China
中国上海市延安西路65号上海国际贵都大饭店办公楼405单元
Phone: +86-21-62489820
Fax: +86-21-62489821

IntechOpen